Observation of the Decay $\Xi^0 \to \Sigma^+ e^- \overline{\nu}_e$

A. Affolder,[4] A. Alavi-Harati,[12] I. F. Albuquerque,[10] T. Alexopoulos,[12] M. Arenton,[11] K. Arisaka,[2] S. Averitte,[10] A. R. Barker,[5] L. Bellantoni,[7] A. Bellavance,[9] J. Belz,[10] R. Ben-David,[7] D. R. Bergman,[10] E. Blucher,[4] G. J. Bock,[7] C. Bown,[4] S. Bright,[4] E. Cheu,[1] S. Childress,[7] R. Coleman,[7] M. D. Corcoran,[9] G. Corti,[11] B. Cox,[11] M. B. Crisler,[7] A. R. Erwin,[12] R. Ford,[7] A. Golossanov,[11] G. Graham,[4] J. Graham,[4] K. Hagan,[11] E. Halkiadakis,[10] K. Hanagaki,[8] S. Hidaka,[8] Y. B. Hsiung,[7] V. Jejer,[11] J. Jennings,[2] D. A. Jensen,[7] R. Kessler,[4] H. G. E. Kobrak,[3] J. LaDue,[5] A. Lath,[10] A. Ledovskoy,[11] P. L. McBride,[7] A. P. McManus,[11] P. Mikelsons,[5] E. Monnier,[4,*] T. Nakaya,[7] U. Nauenberg,[5] K. S. Nelson,[11] H. Nguyen,[7] V. O'Dell,[7] M. Pang,[7] R. Pordes,[7] V. Prasad,[4] C. Qiao,[4] B. Quinn,[4] E. J. Ramberg,[7] R. E. Ray,[7] A. Roodman,[4] M. Sadamoto,[8] S. Schnetzer,[10] K. Senyo,[8] P. Shanahan,[7] P. S. Shawhan,[4] W. Slater,[2] N. Solomey,[4] S. V. Somalwar,[10] R. L. Stone,[10] I. Suzuki,[8] E. C. Swallow,[4,6] R. A. Swanson,[3] S. A. Taegar,[1] R. J. Tesarek,[10] G. B. Thomson,[10] P. A. Toale,[5] A. Tripathi,[2] R. Tschirhart,[7] Y. W. Wah,[4] J. Wang,[1] H. B. White,[7] J. Whitmore,[7] B. Winstein,[4] R. Winston,[4] J. Y. Wu,[5] T. Yamanaka,[8] and E. D. Zimmerman[4]

(KTeV Collaboration)

[1]*University of Arizona, Tucson, Arizona 85721*
[2]*University of California at Los Angeles, Los Angeles, California 90095*
[3]*University of California at San Diego, La Jolla, California 92093*
[4]*The Enrico Fermi Institute, The University of Chicago, Chicago, Illinois 60637*
[5]*University of Colorado, Boulder, Colorado 80309*
[6]*Elmhurst College, Elmhurst, Illinois 60126*
[7]*Fermi National Accelerator Laboratory, Batavia, Illinois 60510*
[8]*Osaka University, Toyonaka, Osaka 560 Japan*
[9]*Rice University, Houston, Texas 77005*
[10]*Rutgers University, Piscataway, New Jersey 08855*
[11]*The Department of Physics and Institute of Nuclear and Particle Physics, University of Virginia, Charlottesville, Virginia 22901*
[12]*University of Wisconsin, Madison, Wisconsin 53706*

(Received 23 December 1998)

We present the first observation of Ξ^0 beta decay, using the KTeV beam line and detector at Fermilab. We have identified 176 beta decay events after subtracting a 7 event background. Normalization to 41 024 simultaneously collected $\Xi^0 \to \Lambda^0 \pi^0$ decays yields a branching ratio of $\Gamma(\Xi^0 \to \Sigma^+ e^- \overline{\nu}_e)/\Gamma_{\text{total}} = (2.71 \pm 0.22_{\text{statistical}} \pm 0.31_{\text{systematic}}) \times 10^{-4}$. The flavor symmetric quark model calculation agrees with this result. [S0031-9007(99)09086-9]

PACS numbers: 13.30.Ce, 14.20.Jn

We report the first observation of Ξ^0 beta decay, $\Xi^0 \to \Sigma^+ e^- \overline{\nu}_e$, and measurement of its branching ratio (BR). Under d and s quark interchange, this process is the direct analog of the neutron beta decay, $n \to p e^- \overline{\nu}_e$. Thus, in the flavor symmetric quark model, differences between these two decays arise only from the differing particle masses and from the relevant Cabibbo Kobayashi Maskawa [1] matrix elements (V_{us} rather than V_{ud}). In the symmetry limit, the calculated [2] branching ratio is $(2.61 \pm 0.11) \times 10^{-4}$. Flavor symmetry violation effects [3,4] are expected to modify this branching ratio by several percent. The directly measurable final state Σ^+ polarization should allow future precision measurements of form factors, providing additional information on flavor symmetry.

The KTeV beam line and detector at Fermilab were designed [5] for high precision studies of CP violation in the neutral kaon system (E832) and studies of rare decays (E799-II). Since the apparatus was situated far from the production target, to reduce backgrounds to K_L decays, only the highest momentum hyperons (from 130 to 600 GeV/c with a mean momentum at 280 GeV/c for Ξ^0) reached it. An intense neutral beam, powerful particle identification, and very good resolution for both charged particles and photons made it a good facility for the study of Ξ^0 decays. During data taking, about 5×10^6 Ξ^0 arrived at the decay volume each day. The data presented here were collected during two months of E799-II data taking in 1997 and correspond to 20% of all the hyperon data taken in 1997.

An 800 GeV/c proton beam, with up to 5×10^{12} protons per 19 s Tevatron spill every minute, was targeted at a vertical angle of 4.8 mrad on a 1.1 interaction length (30 cm) BeO target. Photons were converted by 7.6 cm

of lead immediately downstream of the target. Charged particles were removed further downstream by dipole magnets. Collimators defined two 0.25 μsr neutral beams that entered the KTeV apparatus (Fig. 1) 94 m downstream from the target. The 65 m vacuum ($\sim 10^{-6}$ Torr) decay region extended to the first drift chamber.

The charged particle spectrometer consisted of a dipole magnet surrounded by four (1.28×1.28 m^2 to 1.77×1.77 m^2) drift chambers (DC1–4) with ~ 100 μm position resolution in both horizontal and vertical views. To reduce multiple scattering, helium filled bags occupied the spaces between the drift chambers. In E799-II, the magnetic field imparted a ± 205 MeV/c horizontal momentum component to charged particles, yielding a momentum resolution of $\sigma(P)/P = 0.38\% \oplus 0.016\%\ P$ (GeV/c) (quadratic sum). The magnet polarity was flipped on a daily basis.

The electromagnetic calorimeter (ECAL) consisted of 3100 pure CsI crystals. Each crystal was 50 cm long (27 radiation lengths, 1.4 interaction lengths). Crystals in the central region (1.2×1.2 m^2) had a cross-sectional area of 2.5×2.5 cm^2 while those in the outer region [$(1.2-1.9) \times (1.2-1.9)$ m^2] had a 5×5 cm^2 area. After calibration, the ECAL energy resolution was 0.85% for the electron momentum spectrum in this analysis. The position resolution was ~ 1 mm.

Nine photon veto assemblies detected particles leaving the fiducial volume. Two scintillator hodoscopes in front of the ECAL were used to trigger on charged particles. Another scintillator plane (hadron-anti), located behind both the ECAL and a 10 cm lead wall, acted as a hadron shower veto. The hodoscopes and the ECAL detectors had two holes (15×15 cm^2 at the ECAL) and the hadron-anti had a single 64×34 cm^2 hole to let the neutral beams pass through without interaction. Charged particles passing through these holes were detected by 16×16 cm^2 scintillators (hole counters) located along each beam line in the hole region just downstream of the hadron-anti.

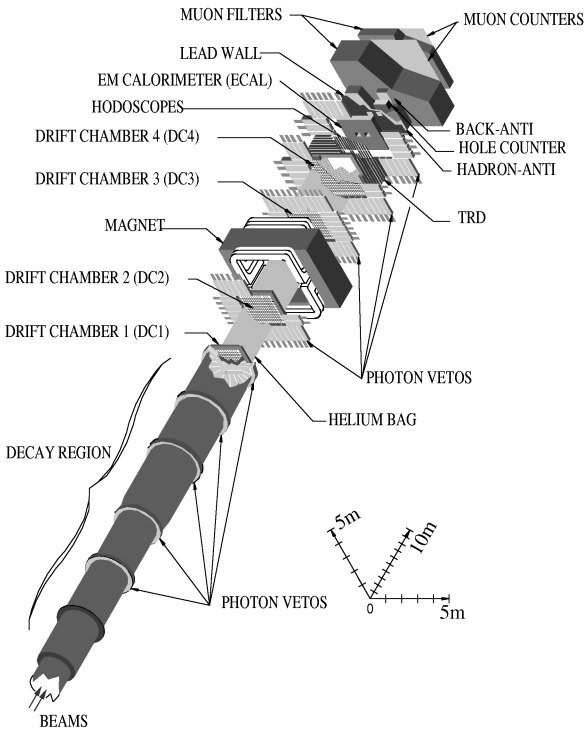

FIG. 1. The KTeV apparatus as configured for this measurement. The transition radiation detector (TRD), muon, and back-anti systems are not used in this analysis.

The beta decay, $\Xi^0 \to \Sigma^+ e^- \overline{\nu}_e$ followed by $\Sigma^+ \to p\pi^0$, has a topology similar to the dominant Ξ^0 decay sequence, $\Xi^0 \to \Lambda^0 \pi^0$ followed by $\Lambda^0 \to p\pi^-$, which was used for normalization. Both sequences had a high momentum (>100 GeV/c) positive track (proton) which remained in or near the neutral beam region, a second lower momentum negative track (π^- or e^-), and two neutral (i.e., unassociated to any track) ECAL energy clusters (photons from a π^0). The beta decay was distinguished by the presence of a decay electron and by its different vertex structure.

The basic hyperon trigger thus required a signal in one of the hole counters with corresponding signals from DC1 and DC2, one or more hodoscope signals, no activity in the photon veto system (to veto events with photons escaping the fiducial volume), and a trigger signal from a special hardware stiff track trigger (STT) element designed to select high momentum (>50 GeV/c) tracks based on hit positions in the DC1–4 horizontal views. This basic hyperon trigger, prescaled by 50, provided our $\Xi^0 \to \Lambda^0 \pi^0$ candidates for normalization. The beta decay trigger, in addition to the basic hyperon trigger criteria, further required one to four in-time (within a 19 ns wide time slice) energy clusters [6] with a total energy of at least 18 GeV in the ECAL, minimal hadronic shower activity in the hadron-anti (<2.5 times the minimum ionizing particle energy), and hits in the DC1–4 vertical views consistent with two tracks. The beta decay trigger was prescaled by 2 to fit in its limited trigger bandwidth with respect to the kaon triggers. Finally, to allow studies of the basic hyperon trigger and of the beta decay trigger, there was a minimum bias trigger, prescaled by 20 000, that required signals only in the hodoscopes and in the hole counters.

In contrast to other hyperon beta decays, the absence of a competing two-body decay containing a Σ^+ eliminated a major background to our signal. Therefore, the possible backgrounds were as follows: (a) $K_L^0 \to \pi^\pm e^\mp \nu_e$, $\Lambda^0 \to p\pi^-$, or $\Lambda^0 \to p e^- \overline{\nu}_e$ decays with, in each case, two accidentally coincident photons; (b) $K_L^0 \to \pi^0 \pi^\pm e^\mp \nu_e$ or $K_L^0 \to \pi^+ \pi^- \pi^0$; and (c) $\Xi^0 \to \Lambda^0 \pi^0$ with either $\Lambda^0 \to p\pi^-$ or $\Lambda^0 \to p e^- \overline{\nu}_e$ as subsequent decays, or $\Xi^0 \to \Sigma^0 \gamma$ with $\Sigma^0 \to \Lambda^0 \gamma$ followed by $\Lambda^0 \to p\pi^-$. As described below, clustering, kinematic, and event topology selections strongly suppressed these backgrounds that are due either to out of time activities (a) or to a misinterpretation of the decay strings (b) and (c). The primary

residual background was $\Xi^0 \to \Lambda^0\pi^0$ followed by $\Lambda^0 \to p$ + anything. Background investigations and acceptance calculations were carried out with a detailed Monte Carlo simulation of the beam and detector.

During reconstruction and analysis, we sought to minimize event losses and to treat beta and $\Lambda^0\pi^0$ candidates as similarly as possible. All events were required to have at least two neutral ECAL clusters (π^0 candidate) above 3 GeV and separated by more than 15 cm, and a low momentum negative track (2.5–50 GeV/c for e^- and 2.5–75 GeV/c for π^-) pointing outside of the beam hole regions of the ECAL. The proton was identified by a high momentum (110–400 GeV/c) positive track pointing to one of the beam holes of the ECAL. To reject K^0 backgrounds, the ratio of the positive track momentum over the negative track momentum was required to be greater than 3.5. Identical track quality and fiducial requirements were imposed on all events.

Candidate $\Xi^0 \to \Sigma^+ e^- \overline{\nu}_e$ reconstruction proceeded from downstream to upstream. The secondary Σ^+ decay vertex was located, with a longitudinal resolution of 0.4 m, at the point along the proton track where the two highest energy neutral ECAL clusters matched the π^0 mass. The primary Ξ^0 vertex was then defined at the point of closest approach of the extrapolated Σ^+ path and the negative track. To remove $\Xi^0 \to \Lambda^0\pi^0$ background candidates, a $\Xi^0 \to \Lambda^0\pi^0$ hypothesis, described below, was used to reject candidates with a reconstructed $\Lambda^0\pi^0$ mass below 1.33 GeV/c^2.

All vertices were required to fall within the decay region fiducial volume (95–150 m), and primary Ξ^0 vertices were required to lie within a neutral beam. We eliminated primary Λ^0 or K^0 two-body decays by rejecting events with charged vertex transverse momentum squared less than 0.001 (GeV/c)^2. To enforce correct vertex geometry and to reduce further the primary Λ^0 or K^0 decay backgrounds, each secondary vertex was required to be 1–20 m downstream of the primary vertex. Further requirements were imposed on reconstructed Ξ^0 momentum (160–500 GeV/c) and decay distance (<10 lifetimes).

Only those events in the beta decay trigger sample which contain an e^-, identified by the deposition of more than 90% of its energy in the ECAL, were retained. We also required a suitable $\Sigma^+ e^-$ invariant mass (1.20–1.32 GeV/c^2) and a missing transverse momentum which was (within a 25 MeV/c uncertainty) less than the reconstructed neutrino momentum in the Ξ^0 rest frame.

The $p\pi^0$ invariant mass distribution for the 235 remaining candidates is shown in Fig. 2. A clear Σ^+ mass peak is apparent, containing 183 events within ± 15 MeV/c^2 (± 3 standard deviations) of the Σ^+ mass [7]. The gray region of Fig. 2 is the distribution for the primary predicted background, from Ξ^0 decay, normalized to the beam flux measured from the normalization sample. The tail of this distribution was estimated to contribute seven events under the mass peak. After subtracting this known

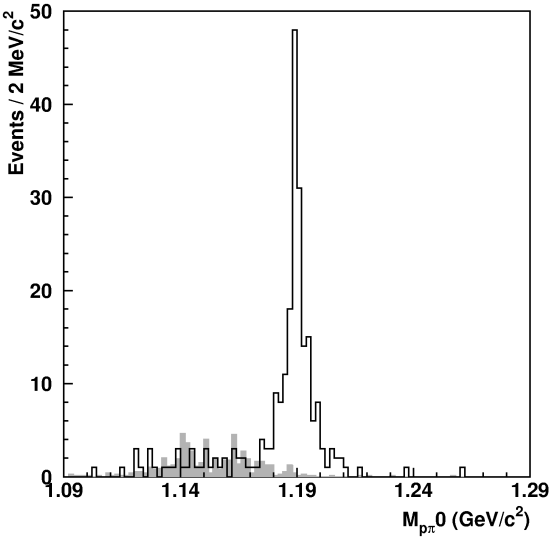

FIG. 2. Reconstructed $p\pi^0$ invariant mass distribution for the Ξ^0 beta decay candidates. Superimposed in gray is the simulated background from $\Xi^0 \to \Lambda^0\pi^0$ decays with $\Lambda^0 \to p$ + anything.

background from the mass distribution, the residual background was estimated to be negligible by counting events in two 15 MeV/c^2 mass regions on either side of the peak (1.155–1.170;1.21–1.225) yielding a total sample of 176 ± 14 $\Xi^0 \to \Sigma^+ e^- \overline{\nu}_e$ events. The reconstructed Σ^+ and Ξ^0 decay distance distributions matched those predicted from known lifetime values. Distributions such as the proton and electron momentum spectra in the laboratory frame and the neutrino momentum spectrum in the Ξ^0 rest frame (Fig. 3) for simulated $\Xi^0 \to \Sigma^+ e^- \overline{\nu}_e$ decays all agreed with the data.

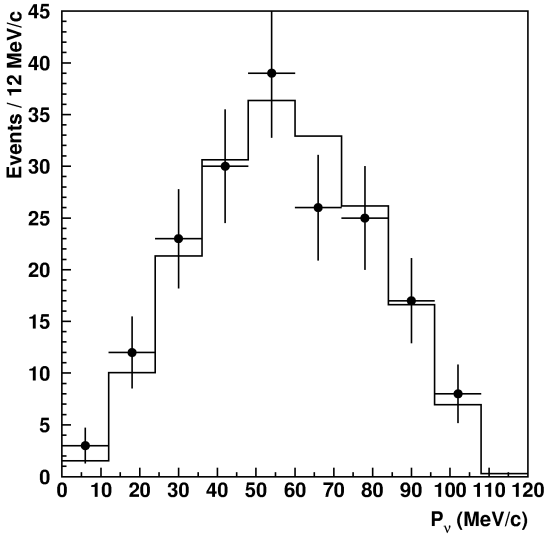

FIG. 3. Neutrino momentum spectrum in the Ξ^0 rest frame. Points are data with statistical uncertainties, and the histogram is our Monte Carlo simulation normalized to the same number of events. The acceptance has little effect on this distribution.

The $\Xi^0 \to \Lambda^0\pi^0$ candidate events were similarly identified in the basic hyperon trigger sample with a $\Xi^0 \to \Lambda^0\pi^0$ hypothesis. The two charged tracks were fit to locate the Λ^0 vertex. The reconstructed Λ^0 mass was required to be within ± 10 MeV/c^2 (± 5 standard deviations) of its value [7]. The primary Ξ^0 decay vertex was then located along the extrapolated Λ^0 path using the π^0 constraint. Accepted events were required to have less than 80% of the negative track (π^-) energy deposited in the ECAL and to have a $\Lambda^0\pi^0$ invariant mass within ± 15 MeV/c^2 (± 5 standard deviations) of the Ξ^0 mass [7]. The resulting normalization sample contained 41 024 $\Xi^0 \to \Lambda^0\pi^0$ events. Again, kinematic distributions for simulated events agreed well with the data. The level of background in this sample was negligible.

Events from the minimum bias trigger and from the basic hyperon trigger were used to determine the beta decay and the basic hyperon trigger efficiencies and to validate aspects of the simulation. For the trigger elements unique to the beta decay trigger, a combined efficiency of $\epsilon = 0.98 \pm 0.01$ was obtained. For the trigger elements common to both triggers, only the STT had significant potential to create noncanceling effects. These effects arose because the DC1–4 wires used by the STT were the limiting aperture for protons and because the STT rejected events with more than one particle hitting these wires. We compared $\Lambda^0 \to p\pi^-$ and $\Xi^0 \to \Lambda^0\pi^0$ minimum bias trigger events with a Monte Carlo simulation. The STT absolute efficiency was $31 \pm 3\%$ and its relative acceptance was 1.0 ± 0.1. We thus included a 10% systematic uncertainty contribution for the STT. When each of the selection criteria was systematically varied, no statistically significant variations were detected. We also found that the beta decay acceptance had a negligible dependence on the form factor values used in the simulation. We therefore assigned a combined 5% systematic uncertainty to our simulation of the relative acceptance. We also ascribed a ± 3 events systematic uncertainty to the background subtraction to allow for possible inadequacies in the subtraction method. Combined in quadrature, these contributions yielded a 11.3% net systematic uncertainty.

Monte Carlo studies gave a relative acceptance of $\epsilon \times \mathrm{A}(\Xi^0 \to \Sigma^+ e^- \overline{\nu}_e)/\mathrm{A}(\Xi^0 \to \Lambda^0\pi^0) = 0.98 \times 0.0253/0.0318 = 0.780 \pm 0.011_{\mathrm{stat}} \pm 0.088_{\mathrm{syst}}$. This includes losses due to detector geometry, trigger efficiencies, event reconstruction, and particle identification with their corresponding statistical and systematic uncertainties. Using this relative acceptance, the two event samples with their prescale factors, and known branching ratios [7], we found $B(\Xi^0 \to \Sigma^+ e^- \overline{\nu}_e) = \Gamma(\Xi^0 \to \Sigma^+ e^- \overline{\nu}_e)/\Gamma_{\mathrm{total}} = (2.71 \pm 0.22 \pm 0.31) \times 10^{-4}$. The first uncertainty is statistical and the second is systematic. As a further global test, we calculated BR values separately for each beam, for each analysis magnet polarity, and for the early and later halves of the data taking. In every case, the results were statistically consistent.

In summary, we observed Ξ^0 beta decay for the first time and measured its branching fraction. The clean beta decay signal (~4% total background) implies that we have suppressed the dominant Ξ^0 decay mode by more than 10^5. This branching ratio result does not distinguish between the exact flavor symmetry calculation and lower values based on flavor symmetry violation analyses [3,8]. We have now accumulated 5 times more events with improved triggering and systematic uncertainties, making possible future studies of decay angular distributions as well as a more accurate branching ratio determination that may distinguish between models.

We thank A. Garcia, A. Manohar, and J. Rosner for many helpful discussions. We gratefully acknowledge the support and effort of the Fermilab staff and the technical staffs of the participating institutions for their vital contributions. This work was supported in part by the U.S. Department of Energy, The National Science Foundation, and The Ministry of Education and Science of Japan. In addition, A. R. B., E. B., and S. V. S. acknowledge support from the NYI program of the NSF; A. R. B. and E. B. from the Alfred P. Sloan Foundation; E. B. from the OJI program of the DOE; and K. H., T. N., and M. S. from the Japan Society for the Promotion of Science.

*On leave from C.P.P. Marseille/C.N.R.S., France.
To whom correspondence should be addressed.
Electronic address: monnier@hep.uchicago.edu

[1] N. Cabibbo, Phys. Rev. Lett. **10**, 531 (1963); M. Kobayashi and T. Maskawa, Prog. Theor. Phys. **49**, 652 (1973). See also M. Gell-Mann and M. Levy, Nuovo Cimento **16**, 705 (1960); Z. Maki, M. Nakagawa, and S. Sakata, Prog. Theor. Phys. **28**, 870 (1962).

[2] We have used numerical values from Ref. [7] and the notation and formulas of Ref. [4] for this calculation ($f_1 = 1, |V_{us}| = 0.2196 \pm 0.0023$, $g_1/f_1 = 1.2670 \pm 0.0035$, $f_2/f_1 = 2.60$, $g_2 = 0$, $M_V = 970$ MeV/c^2, $M_A = 1250$ MeV/c^2). The uncertainties come primarily from the Ξ^0 mass and lifetime.

[3] See, for example, R. Flores-Mendieta, E. Jenkins, and A. V. Manohar, Phys. Rev. D **58**, 094028 (1998); A. Garcia, R. Huerta, and P. Kielanowski, Phys. Rev. D **45**, 879 (1992); C. Avenarius, Phys. Lett. B **272**, 71 (1991); M. Roos, Phys. Lett. B **246**, 179 (1990); P. G. Ratcliffe, Phys. Lett. B **365**, 383 (1996); L. J. Carson, R. J. Oakes, and C. R. Willcox, Phys. Rev. D **37**, 3197 (1988), wherein flavor symmetry violation is considered in a variety of contexts.

[4] A. Garcia and P. Kielanowski, in *The Beta Decay of Hyperons*, Lecture Notes in Physics Vol. 222 (Springer-Verlag, Berlin, 1985).

[5] K. Arisaka *et al.*, "KTeV (Kaons at the Tevatron) Design Report," Fermilab Report No. FN-580, 1992.

[6] C. Bown *et al.*, Nucl. Instrum. Methods Phys. Res., Sect. A **369**, 248 (1996).

[7] Particle Data Group, C. Caso *et al.*, Eur. Phys. J. C **3**, 1 (1998).

[8] A. Manohar and A. Garcia (private communication).